2021

Interactions between Refrigerant Charge and Other Installation Faults on the Behavior of a Residential Heat Pump in Cooling Mode

Yifeng Hu
University of Nebraska-Lincoln, United States of America, yifeng.hu@huskers.unl.edu

David P. Yuill

Seyed Ali Rooholghodos

Interactions between Refrigerant Charge and Other Installation Faults on the Behavior of a Residential Heat Pump in Cooling Mode

Yifeng HU*, David P. YUILL, Seyed Ali ROOHOLGHODOS
Durham School of Architectural Engineering and Construction, University of Nebraska – Lincoln
Omaha, NE 68182, USA
yifeng.hu@huskers.unl.edu

*Corresponding author

ABSTRACT

The effects of refrigerant charge (CH) faults have been intensively investigated over the past three decades. However, the effect of CH faults in the presence of other faults, like the presence of non-condensable gas (NC), has been seldom studied. The patterns of the effect of CH faults on a system with other faults could be different from that on a fault-free system, which could degrade the performance of fault diagnostic tools and cause improper charging by technicians during installation or service of systems in the field. To address this problem, four common installation faults - improper evaporator airflow (EA), liquid line restrictions (LL), CH, and NC faults were imposed on an 18 SEER residential heat pump with a TXV metering device both individually and simultaneously, and the system was tested in a laboratory. First, the individual impacts of undercharge (UC) and overcharge (OC) on the performance of the system were evaluated under four different operating conditions. Then, the impacts of CH faults in the presence of the other three faults, both singly and in combinations, were examined at one operating condition. Under single CH fault conditions, the cooling capacity decreased for UC faults but was almost unchanged for OC faults, while the COP decreased for both UC and OC faults. In combination with other faults, the trend for UC faults is the same as those for the fault-free system. However, the OC fault can ameliorate the impacts of other faults on capacity, particularly a severe LL fault (LL32). The effect on COP for OC faults depends on fault type and intensity. For example, the COP with an OC fault decreased in the presence of light LL fault (LL22) but increased in the presence of a more severe LL fault (LL32). The variations of indicator variables such as refrigerant temperatures under different fault conditions are also presented.

1. INTRODUCTION

Improper refrigerant charge (CH), including undercharge (UC) and overcharge (OC), is an important fault that can occur in air conditioning systems. To evaluate the impacts of CH faults on the performance of the system, several laboratory experimental studies (Farzad, 1990; O'Neal and Farzad, 1990; Farzad and O'Neal, 1991, 1993; Neal and O'Neal, 1992; Rossi and Braun, 1997; Breuker and Braun, 1998a, b; Chen and Braun, 2000, 2001; Goswami et al., 2001; Harms et al., 2003; Shen et al., 2006, 2009, 2011; Kim et al., 2006, 2009; Payne et al., 2009; Raj and Lal, 2010; Yoon et al., 2011; Palmiter et al., 2011; Kim and Braun, 2012; Mowris et al., 2012; Cho et al., 2014; Domanski et al., 2014; Du et al., 2016; Hu et al., 2021a, b) have investigated this fault. Mehrabi and Yuill (2017) analyzed the previous studies to generalize the effects of CH faults across systems, and found the effects to be quite homogeneous.

Several studies (Li, 2004; Li and Braun, 2007a, b; Wichman and Braun, 2009; Shen et al., 2011; Palmiter et al., 2011; Wang et al., 2016; Kim and Braun, 2020; Hu et al., 2021b) have investigated simultaneous faults. Li (2004) and Li and Braun (2007a, b) investigated multiple simultaneous faults of UC, VL, CA, EA, and LL on an RTU in the field with uncontrollable operating conditions. The maximum degradation found in this study was 39% for capacity and 35% for COP. Wichman and Braun (2009), Shen et al. (2011), Palmiter et al. (2011), and Kim and Braun (2020) each investigated double simultaneous faults in the laboratory. Wichman and Braun (2009) studied double faults of UC with EA, CA, VL, and LL on a walk-in cooler and of EA with VL, CA, LL, and UC on a walk-in freezer. They reported up to 40% reduction in capacity on the cooler with UC at 50% and LL at level 5. Shen et

al. (2011) and Palmiter et al. (2011) each investigated simultaneous CH and IA faults on a split heat pump system. A maximum reduction of 20% in capacity with IA at 63% and CH at 70% in heating mode was found in Shen et al. (2011), and a maximum reduction of 10% in COP with IA at 75% and CH at 49% in cooling mode was found in and Palmiter et al. (2011). Wang et al. (2016) conducted tests to determine the fault impacts of two combined faults on an RTU. The combinations included CA + VL and CA + EA. Capacity reductions up to 14% and COP reductions up to 16% were reported for CA + VL. With a combination of severe EA (50% reduction) and CA (30% reduction), the capacity was reduced by 14% and COP by 33%. Kim and Braun(2020) also considered combinations of two faults, from among CH, VL, LL, CA, and EA, on an RTU. This was done to validate an FDD method, the paper didn't include measurement results of the fault impacts on operating parameters.

Hu et al. (2021a, b, c) tested a 4-ton split system heat pump equipped (rated 18 SEER, using R410A refrigerant, equipped with a TXV) in cooling mode. Four different types of common faults – improper evaporator airflow (EA), improper refrigerant charge (CH), liquid line restrictions (LL), and the presence of non-condensable gas (NC) in the refrigerant– were imposed individually at four operating conditions, and were imposed simultaneously for one operating condition. The performance effects of single CH faults (Hu et al., 2021a) are similar to the previous studies (Kim et al., 2006, 2009; Domanski et al., 2014; Cho et al., 2014; Du et al., 2016) but less sensitive to fault intensity. For example, at 80% CH level, the COP decreased by only 1%, on average, for the four different operating conditions, while Mehrabi and Yuill (2017) found a reduction of about 5% at this charge level for the multiple systems they studied. The performance impacts of simultaneous double, triple, and quadruple faults are examined and compared to the fault-free condition in Hu et al. (2021b). For instance, the COP decreased by 24% and capacity decreased by 30% with a combination of CH at 70% and LL at 32%; the COP went down by 34% and capacity went down by 38% with the quadruple fault combination of CH at 70%, EA at 60%, LL at 32%, and NC at 49%.

In the current paper, instead of investigating the relationship between simultaneous faults and the fault-free condition, we focus on examining the effects of CH faults in the presence of one, two, and three other faults. For example, how did the CH faults impact the performance of the system when the system was already faulted with an LL fault? Is the impact different from that of CH faults on a fault-free system? Does superposition apply with fault combinations, or is there synergy or cancellation in some cases? In addition, the variations of indicator variables, such as refrigerant subcooling under different fault conditions, are also presented. This perspective on fault impacts gives new insight into the importance of charge verification within the context of the inevitability of other faults, and also provides a basis for FDD developers to improve the performance of their diagnostics within this context, by showing how features from one fault can affect features of another.

2. Methodology

2.1 Test apparatus

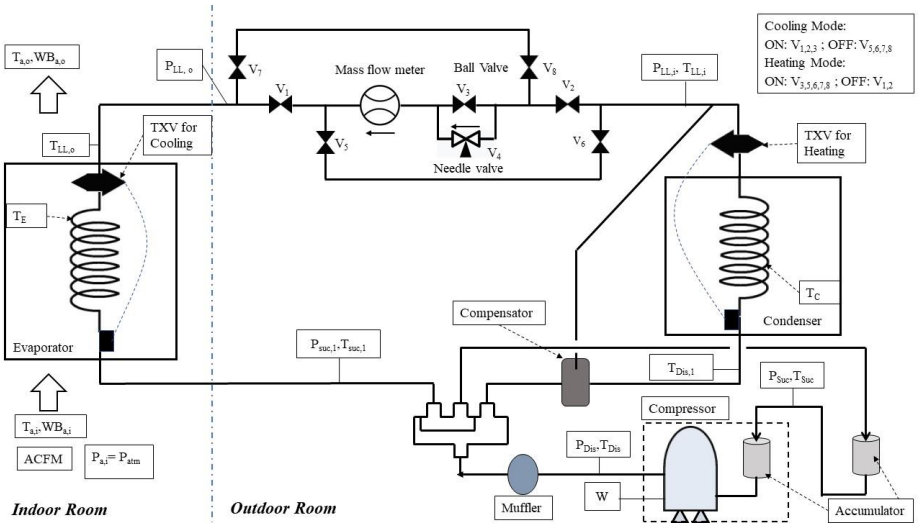

Figure 1: Experimental setup with the tested heat pump unit in cooling mode (Hu et al., 2021a)

Experiments were carried out on an R410A split system heat pump with a rated 12.9 kW (3.67 tons) capacity, and the 18 SEER. The system has a rotary compressor, a compensator, a muffler, two TXVs, two accumulators, two plate-fin heat exchangers. The experimental setup added a refrigerant mass flow sensor and a system of valves for imposing LL faults and switching modes. Details about the setup and test procedures can be found in Hu et al., (2021a).

2.2 Test matrix

The single faults were imposed in four different operating conditions (shown in Table 1), while the simultaneous faults were only implemented under the "A" operating condition of the AHRI Standard 210/240 (2017) because the trends of single fault impacts under the four different operating conditions were found to be very similar. The EA and CH faults each have four fault intensities (including the fault-free condition of 100%), and LL and NC each have three fault intensities (including the fault-free condition of 0%). Fault combinations are represented in figures, using the notation in Table 2. The manufacturer's limit recommends a limit of 105 °C discharge line temperature, so four combinations of triple faults, and twelve quadruple fault combinations could not be tested. Therefore, there are 117 simultaneous fault combinations (37 double, 56 triple, and 24 quadruple) presented in results.

Table 1: Test conditions (Hu et al., 2021a)

Test Condition	Indoor room		Outdoor room
	Dry-bulb temperature °C (°F)	Wet-bulb temperature °C (°F)	Dry-bulb temperature °C (°F)
A	26.7 (80.0)	19.4 (67.0)	35.0 (95.0)
B	26.7 (80.0)	19.4 (67.0)	27.8 (82.0)
C	26.7 (80.0)	19.4 (67.0)	40.5 (105.0)
D	26.7 (80.0)	<13.3 (<56.0)	35.0 (95.0)

Table 2: Fault intensity and notation

Fault categories			
Fault	**Intensities (%)**	**Intensity definition**	**Notation**
EA	60, 80, 100, 120	% of the nominal evaporator airflow	EA60, EA80, EA100, EA120
CH	70, 80,100,120	% of the nominal charge mass	CH70, CH80, CH100, CH120
LL	0, 22, 32	Ratio of liquid line pressure drop to compressor pressure lift at the A condition	LL0, LL22, LL32
NC	0, 49, 105	Ratio of injected nitrogen pressure at 35 °C to atmospheric pressure	NC0, NC49, NC105

2.3 Methods

To analyze the performance impact on a system with a specific fault in the presence of other faults, we defined the relative performance as:

$$\rho_{CH} = \frac{R_{CH+others} - R_{others}}{R_{others}} \times 100\% \quad (1)$$

where ρ_{CH} represents the relative performance impact of CH faults when imposed on a system with other faults, and R represents a performance parameter. For example, if a system has a COP of 3.0 with some combination of EA, LL, and NC faults, and a CH fault is imposed on top of those faults, resulting in COP of 2.7, then:

$$\rho_{CH} = \frac{2.7-3.0}{3.0} \times 100\% = -10\%$$

The results in Figure 3 to Figure 8 use this concise representation of CH fault impacts.

3. RESULTS AND DISCUSSION

3.1 Single Faults

Figure 2 shows the impact of CH faults alone on the normalized cooling capacity and COP at four operating conditions. The cooling capacity had small variations at the 120% CH level, decreased by 3-5% at 80% CH, and decreased by 7-12% at 70% CH. CH faults impacted capacity most at the high outdoor temperature condition (C), and least at dry-evaporator coil condition (D). The COP is quite flat within ±20% CH deviation, and even increased by around 1% for the dry-coil condition. Our assumption is that the compensation of the TXV to the UC, and the excess charge storage volume of the accumulators, compensator, and a larger condenser (associated with higher rated efficiency) may contribute to this insensitivity. However, when the system is significantly undercharged, the TXV may become fully open, so that COP and cooling capacity will decrease rapidly.

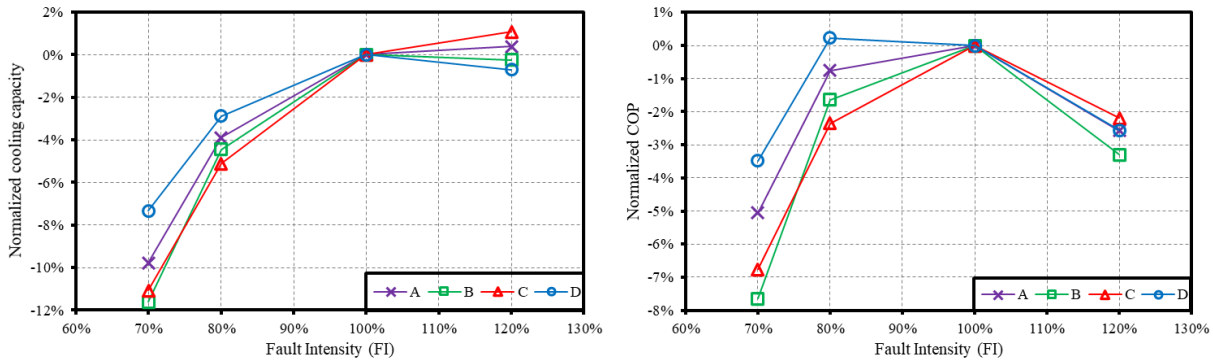

Figure 2: Impacts of CH faults on the normalized cooling capacity (left) and COP (right)

3.2 Double Faults

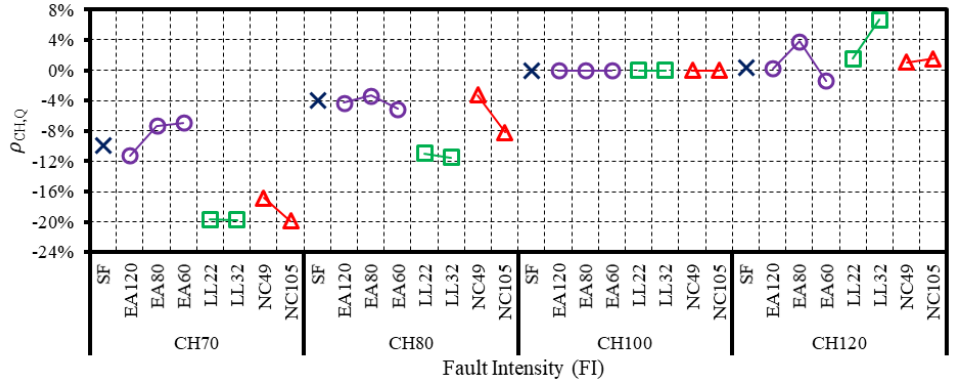

Figure 3: Impacts of CH faults with one other fault on the normalized cooling capacity

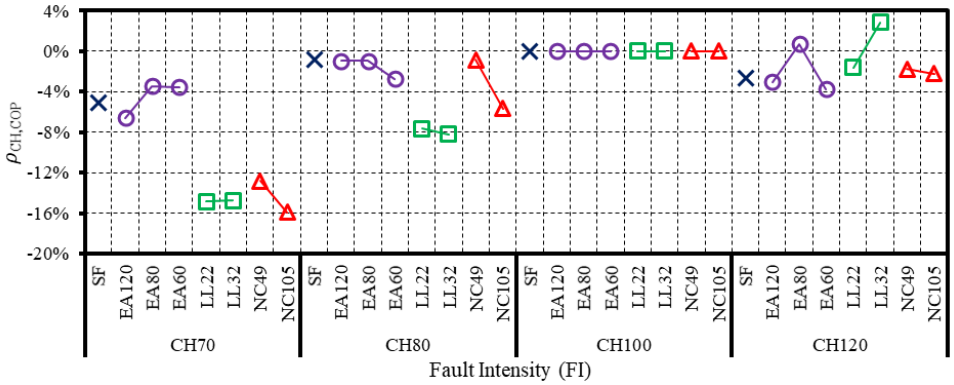

Figure 4: Impacts of CH faults with one other fault on the normalized COP

Figure 3 and Figure 4 present the impacts of CH faults in the presence of one other fault (EA, LL, or NC) on the normalized cooling capacity and COP, respectively. In addition, the effects of single CH faults relative to no fault are also presented as a cross mark (X), and designated with an SF label in each figure, to facilitate comparisons. For example, at CH70 the single fault (SF) reduces COP by about 5%, while for EA60 the addition of CH70 only reduces the COP by about 4% below the COP of the EA60 fault alone. The impacts on capacity of CH faults combined with one other fault have similar trends to single CH fault impacts, except when EA80 or LL32 are combined with OC faults. Figure 4 shows that OC faults can compensate for detrimental effects caused by LL32, and to a lesser extent by EA80. However, UC combinations with other faults always decrease the COP and capacity, but the magnitudes vary depending upon fault types and intensities. In general, combining UC with NC or LL faults increases the impact severity. For example, CH70 combined with LL32 decreased cooling capacity by 19.7% compared to LL32 alone. This is not surprising, since each of these faults tends to starve the evaporator. These types of synergistic effects have also been investigated in detail by Hu et al. (2021b). EA effects tend to be fairly independent of other faults, so that the impact of combinations with CH faults largely follow the superposition principle.

3.3 Triple Faults

a

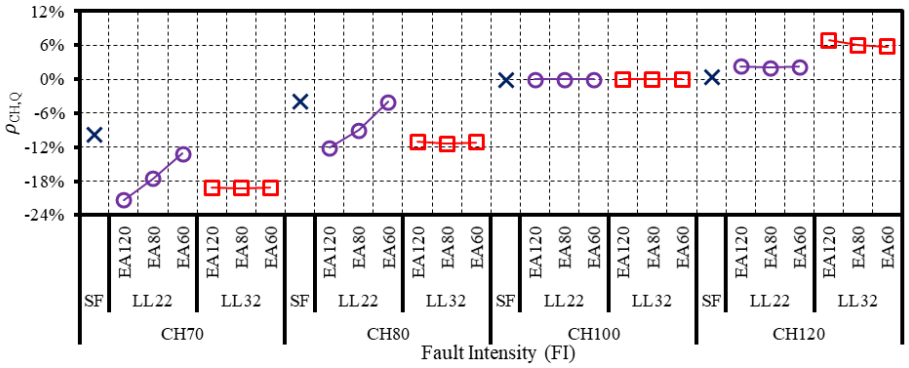

b

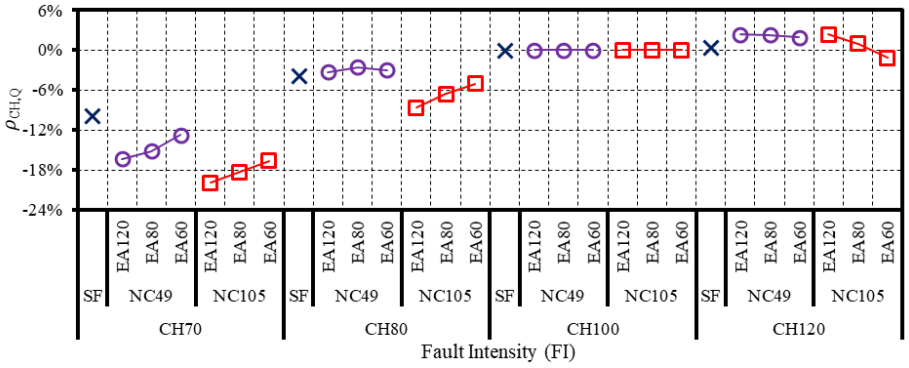

c

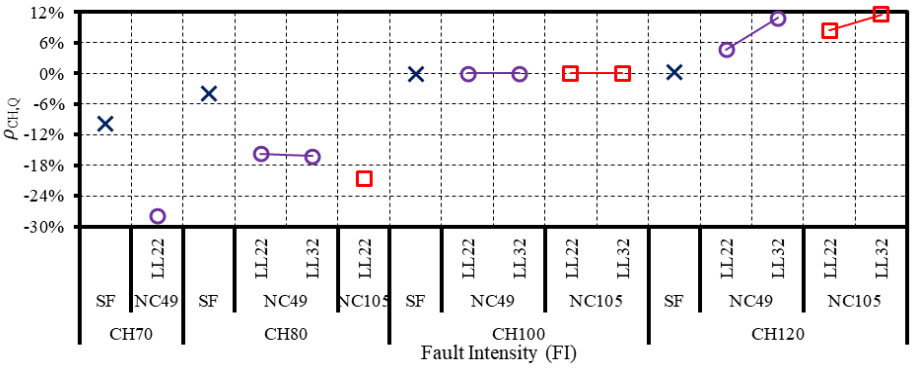

Figure 5: Impacts of CH faults with two other faults on the normalized cooling capacity: a) LL and EA faults, b) NC and EA faults, c) NC and LL faults

Figure 5 shows the impacts on cooling capacity of CH faults combined with pairs of EA, LL, and NC faults. It is split into three parts to accommodate all triple fault combinations. The additional impact of CH faults on the cooling capacity is roughly proportional to the CH level. That is, increasing the CH level always increased the capacity. For instance, with LL32 + NC105, the cooling capacity of CH120 increased by 12%, compared to the nominal CH (CH100). Whether the superposition principle applied the faults depended on the fault combinations and their intensities. For example, with NC49 + EA, the additional effect of CH80 on the capacity was similar to CH80 alone, indicating that the superposition principle applies. However, with NC49 + EA, the additional effect of CH70 on the capacity was higher than that of CH70 alone, indicating a synergistic effect. Synergistic effects are to be expected in scenarios in which the TXV might ameliorate some of the fault impacts (because the combination will tend to force the TXV to full open earlier), and in cases in which the combined faults each primarily impact the same component of the system. Figure 6 shows the impacts on COP of CH faults combined with pairs of EA, LL, and NC faults. The trends and conclusions are similar to the cooling capacity impacts, but are generally smaller in magnitude.

a

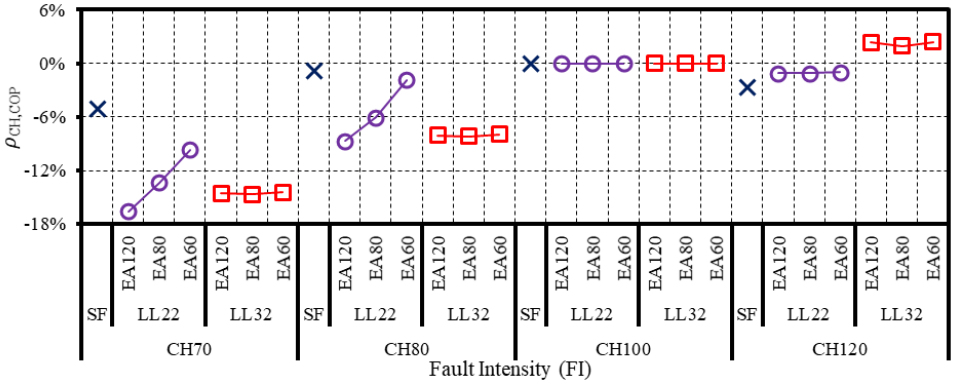

b

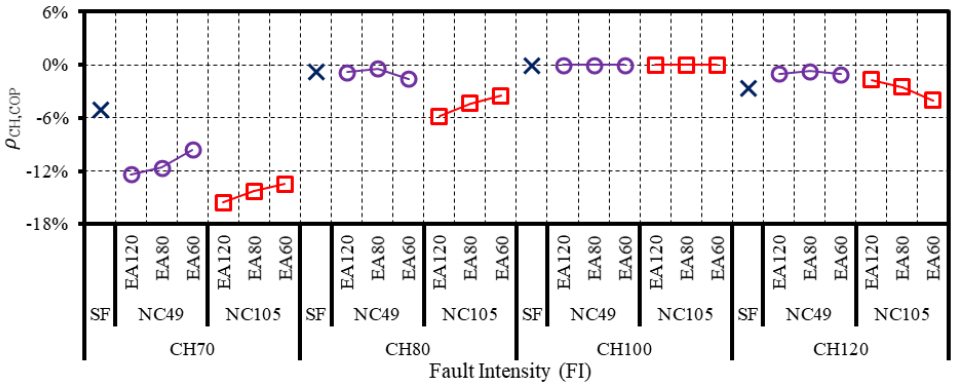

c

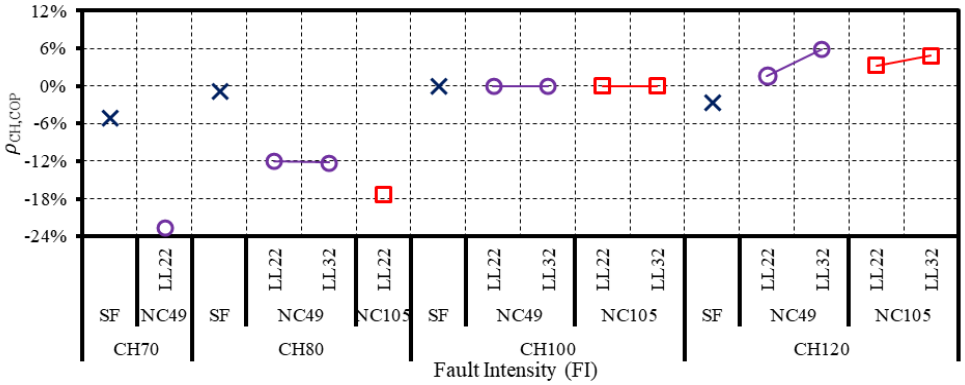

Figure 6: Impacts of CH faults with two other faults on the normalized COP:
a) LL and EA faults, b) NC and EA faults, c) NC and LL faults

3.4 Quadruple Faults

Figure 7 and Figure 8 present the impacts of CH when combined with EA, LL, and NC faults. Some trends are similar to the results for double faults; the capacity is roughly proportional to CH. In most cases, the COP is also proportional to CH, except for the combinations of CH120 + LL22 + EA60 + NC, where the additional charge combines with the other faults to decrease COP relative to CH100. This fault scenario pushes additional charge into the condenser, so that rather than compensating for the other impacts, the overcharge exacerbates them. LL32 tends to starve the evaporator, so that OC consistently compensates for this effect, with cancellation (i.e., > 0) seen on the right side of the plot. The impacts of CH range up to -28.2% on capacity and -22.9% on COP (for the impact of CH70 on the case of LL22 + NC49 + EA120) – a very significant additional impact. A summary of the maximum variations in capacity and COP caused by CH faults combined with zero, one, two, and three faults under "A" rating condition is presented in Table 3.

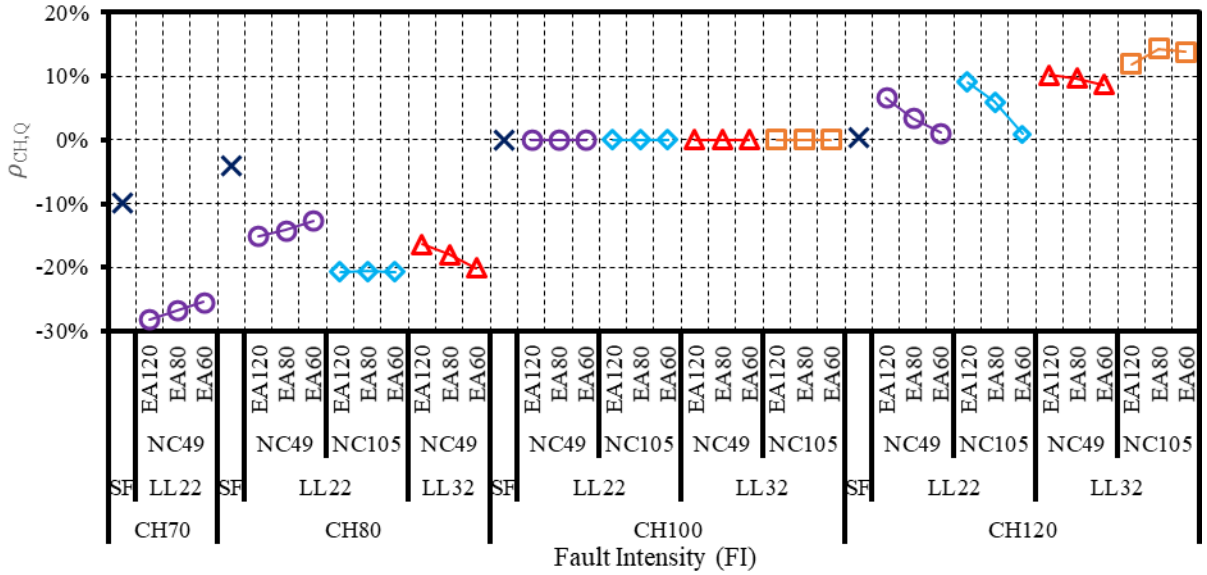

Figure 7: Impacts of CH faults with three other faults on the normalized cooling capacity

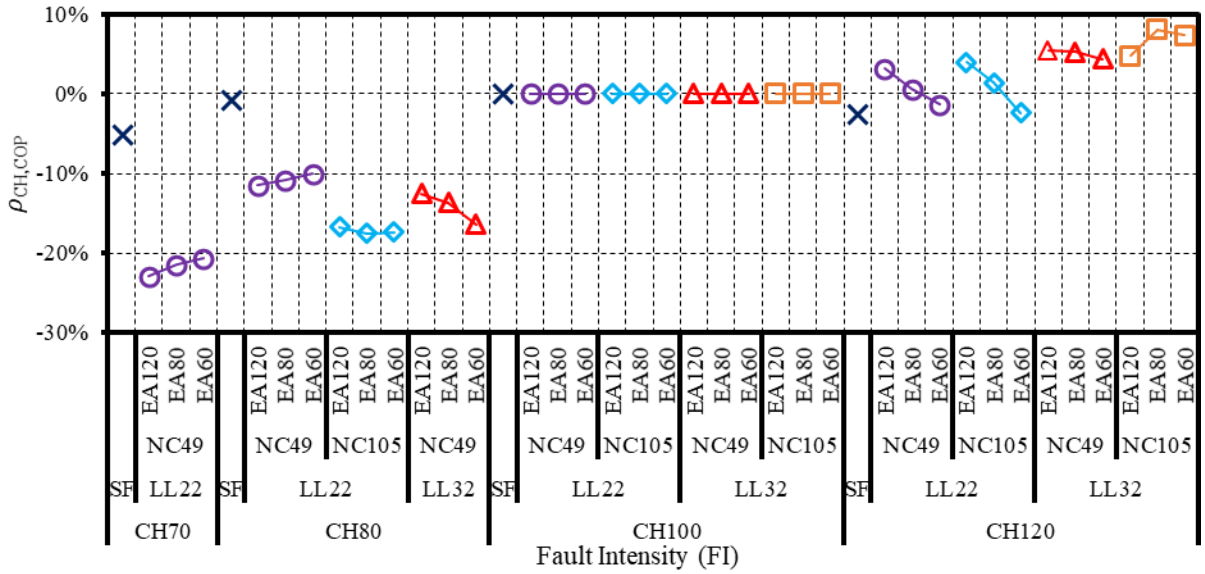

Figure 8: Impacts of CH faults with three other faults on the normalized COP

Table 3: Max. and min. additional impacts caused by adding CH faults to other fault (or no fault) conditions

Fault No. (type)	Combination	Min.	Combination	Max.
Single (capacity)	CH70	-9.8%	CH120	+0.4%
Single (COP)	CH70	5.1%	CH80	-0.8%
Double (capacity)	CH70 + NC105	-19.9%	CH120 + LL32	+6.7%
Double (COP)	CH70 + NC105	-15.9%	CH120 + LL32	+2.9%
Triple (capacity)	CH70 + LL22 + NC49	-27.8%	CH120 + LL32 + NC105	+11.6%
Triple (COP)	CH70 + LL22 + NC49	-22.5%	CH120 + LL32 + NC49	+5.9%
Quadruple (capacity)	CH70 + EA120 + LL22 + NC49	-28.2%	CH120 + EA80 + LL32 + NC105	+14.3%
Quadruple (COP)	CH70 + EA120 + LL22 + NC49	-22.9%	CH120 + EA80 + LL32 + NC105	+8.1%

3.5 Feature analysis

Subcooling is a feature that is commonly used to assess proper charge in TXV-equipped systems. Figure 9 presents the residual subcooling - the difference between double-fault combinations and the fault-free condition (paper length limitation prevents showing additional combinations). Although other fault combinations do impact subcooling, charge has the most severe impacts. The range of residuals for non-charge fault combinations is -0.4 °C (for EA60 + LL22) to +2.7 °C (for EA120 + NC105). In comparison, charge faults give residuals in the -4 to -6 °C range for UC combinations with EA, and up to +5 °C for CH combinations with NC or LL. Still, traditional subcooling-based FDD methods are likely to work poorly in the presence of NC faults, especially at high intensity. A more detailed analysis for residuals of subcooling and other indicator variables for simultaneous faults (double, triple, and quadruple) can be found in Hu and Yuill (2021c).

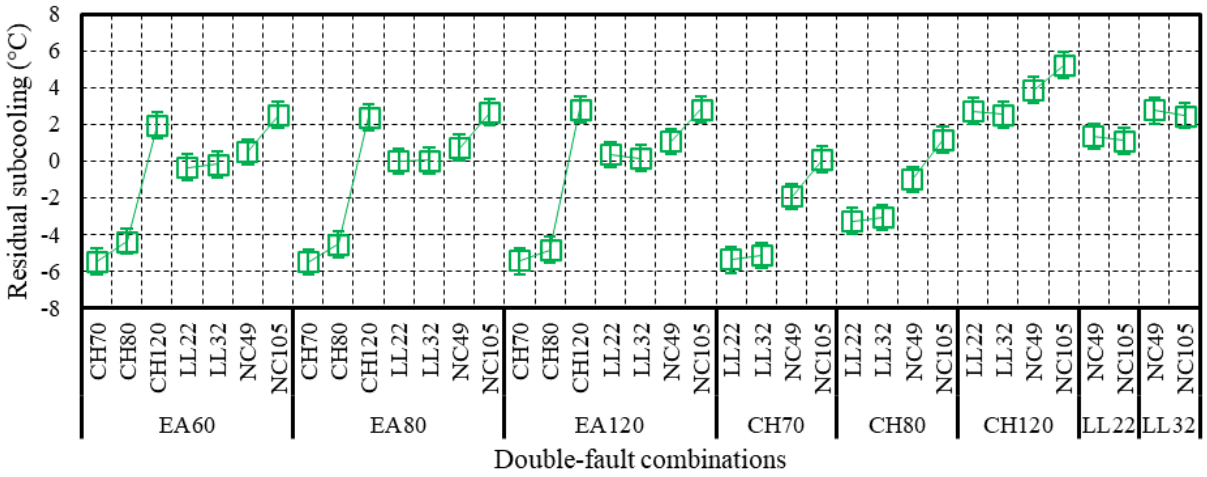

Figure 9: Residuals of subcooling under various double-fault combinations

4. CONCLUSIONS

This paper examined CH fault impacts on the cooling capacity and COP when combined with up to three other fault types. It showed impacts on subcooling for double-fault combinations, as an example feature analysis for combined faults. The following conclusions can be drawn:

- The impact of single CH faults on the performance of the system is comparable for different operating conditions; UC consistently decreased both capacity and COP, OC while had almost no impact on the capacity and decreased the COP.
- When combined with other faults, the trends of impact for UC were still similar to that of UC alone, but the variations in magnitude depended on the fault types and intensities. For example, in the presence of LL or NC, the effect of UC on the performance became more severe, indicating that there are synergistic effects for these fault combinations.

- When combined with other faults, the trends of impact for OC, in most cases, were different from that of OC alone; OC increased the cooling capacity and COP, especially in the presence of LL32, indicating that a canceling effect occurred for fault combinations with OC+ LL.
- Subcooling was mainly controlled by the CH level, even in the presence of LL, EA, or their combinations. However, the presence of NC or its combinations with other faults, increased the subcooling magnitude, especially for NC105. These results showed that subcooling-based FDD and field installation methods for TXV-equipped systems are problematic for some faults combinations, especially with the presence of NC.

NOMENCLATURE

CA	condenser airflow	R	performance parameter
CH	refrigerant charge (including undercharge and overcharge)	SEER	seasonal energy efficiency ratio
COP	coefficient of performance	SF	single faults
EA	evaporator airflow	TXV	thermostatic expansion valve
FDD	fault detection and diagnosis	UC	refrigerant undercharge
FXO	fixed orifice expansion device	VL	compressor valve leakage
IA	indoor airflow (cooling EA, heating CA)	ρ	relative performance
LL	liquid line restriction	**Subscripts**	
NC	non-condensable gas	CH	refrigerant charge
OC	refrigerant overcharge	$\dot{Q}$	cooling capacity

REFERENCES

AHRI (2017). *Performance Rating of Unitary Air-conditioning & Air-source Heat Pump Equipment*. AHRI Standard 210/240-2017, Air-Conditioning & Refrigerant Institute, Arlington, VA, USA.

Chen, B. & Braun, J.E. (2000). Simple fault detection and diagnostics methods for packaged air conditioners. *Proceedings of the 8th International Refrigeration Conference*, Paper 498, West Lafayette, IN, USA.

Chen, B.& Braun, J.E. (2001). Simple rule-based methods for fault detection and diagnostics applied to packaged air conditioners. *ASHRAE Trans., 107*, 847-857.

Breuker, M.S. & Braun, J.E. (1998a). Evaluating the performance of a fault detection and diagnostic system for vapor compression equipment. *HVAC&R Res., 4* (4), 401–425.

Breuker, M.S. & Braun, J.E. (1998b). Common faults and their impacts for rooftop air conditioners. *HVAC&R Res., 4* (3), 303–318.

Cho, J.M., Heo, J., Payne, W.V., Domanski, P.A., (2014). Normalized performance parameters for a residential heat pump in the cooling mode with single faults imposed. *Appl. Therm. Eng., 67* (1), 1–15.

Domanski, P.A., Henderson, H.I., Payne, W.V. (2014). *Sensitivity analysis of installation faults on heat pump performance*. NIST Technical Note 1848, NIST, Gaithersburg, MD, USA.

Du, Z., Domanski, P.A., Payne,W.V. (2016). Effect of common faults on the performance of different types of vapor compression systems. *Appl. Therm. Eng., 98*, 61–72.

EIA (2020). *Annual Energy Outlook 2020 with projections to 2050*. U.S. Energy Information Administration.

Farzad, M. (1990). *Modeling the effects of refrigerant charging on air conditioner performance characteristics for three expansion devices*. Ph.D. Thesis, Texas A&M University, College Station, TX, USA.

Farzad, M. & O'Neal, D.L. (1991). System performance characteristics of an air conditioner over a range of charging conditions. *Int. J. Refrig., 14* (6), 321–328.

Farzad, M. & O'Neal, D.L. (1993). Influence of the expansion valve on air-conditioner system performance characteristics under a range of charging conditions. *ASHRAE Trans., 99* (1), 3–13.

Goswami, D.Y., Ek, G., Leung, M., Jotshi, C.K., Sherif. S.A., Colacino, F. (2001). Effect of refrigerant charge on the performance of air conditioning systems. *Int. J. Energy Res., 25* (8), 741-750.

Harms, T.M., Groll, E.A., Braun, J.E. (2003). Accurate charge inventory modeling for unitary air conditioners. *HVAC&R Res., 9* (1), 55–78.

Hu, Y., Yuill, D.P., Ebrahimifakhar, A., Rooholghodos, A. (2021a). An experimental study of the behavior of a high efficiency residential heat pump in cooling mode with common installation faults imposed. *Appl. Therm. Eng., 184*, 116116.

Hu, Y., Yuill, D.P., Rooholghodos, A., Ebrahimifakhar, A., Chen, Y. (2021b). Impacts of simultaneous operating faults on cooling performance of a high efficiency residential heat pump. *Energy and Build.* (In Press).

Hu, Y., Yuill, D.P. (2021c). Effects of multiple simultaneous faults on characteristic fault detection features of a heat pump in cooling mode. (In Review).

Kim, M, Payne, W.V., Domanski, P.A., Hermes, C.J.L. (2006). *Performance of a Residential Heat Pump Operating in the Cooling Mode with Single Faults Imposed*. NISTIR 7350, NIST, Gaithersburg, MD, USA.

Kim, M., Payne, W.V., Domanski, P.A., Yoon, S.H., Hermes, C.J.L. (2009). Performance of a residential heat pump operating in the cooling mode with single faults imposed. *Appl. Therm. Eng., 29* (4), 770–778.

Kim, W. & Braun, J.E. (2012). Evaluation of the impacts of refrigerant charge on air conditioner and heat pump performance. *Int. J. Refrig., 35* (7), 1805-1814.

Kim, W., Braun, J.E. (2020). Development, implementation, and evaluation of a fault detection and diagnostics system based on integrated virtual sensors and fault impact models. *Energy Build., 226*, 110368.

Li, H. (2004). *A decoupling-based unified fault detection and diagnosis approach for packaged air conditioners*. Ph.D. thesis, School of Mechanical Engineering, Purdue University, West Lafayette, IN.

Li, H. & Braun, J. E. (2007a). A Methodology for Diagnosing Multiple-Simultaneous Faults in Vapor Compression Air Conditioners. *HVAC&R Res., 13* (2), 369-395.

Li, H. & Braun, J.E. (2007b). An overall performance index for characterizing the economic impact of faults in direct expansion cooling equipment. *Int. J. Refrig., 30*, 299-310.

Mehrabi, M. & Yuill, D.P. (2017). Generalized effects of refrigerant charge on normalized performance variables of air conditioners and heat pumps. *Int. J. Refrig., 76*, 367–384.

Mowris, R., Jones, E., Eshom, R. (2012). Laboratory measurements of HVAC installation and maintenance faults. *ASHRAE Trans., 118* (2), 165–172.

Neal, L. & O'Neal, D. L. (1992). The Impact of Residential Air Conditioner Charging and Sizing on Peak Electrical Demand. *Proceedings of the Eighth Symposium on Improving Building Systems in Hot and Humid Climates*, Dallas, TX, USA.

O'Neal, D. L. & Farzad, M. (1990). The effect of improper refrigerant charging on the performance of an air conditioner with capillary tube expansion. *Energy and Build., 14* (4), 363-371.

Payne, W.V., Yoon, S.H., Domanski, P.A. (2009). *Heating mode performance measurements for a residential heat pump with single-faults imposed*. Technical Note 1648, NIST, Gaithersburg, MD, USA.

Palmiter, P., Kim, J.H, Larson, B., Francisco, P.W., Groll, E.A., Braun, J.E. (2011). Measured effect of airflow and refrigerant charge on the seasonal performance of an air-source heat pump using R-410A. *Energy and Build., 43*, 1802–1810.

Raj, M.H. & Lal, D.M. (2010). An experimental analysis of the effect of refrigerant charge level and outdoor condition on a window air conditioner. *Therm. Sci., 14* (4), 1121–1138.

Rossi, T.M. & Braun, J.E. (1997). A Statistical, Rule-based Fault Detection and Diagnostic Method for Vapor Compression Air Conditioners. *HVAC&R Res., 3* (1), 19-37.

Shen, B., Braun, J.E., Groll, E.A. (2006). A method for tuning refrigerant charge in modeling off-design performance of unitary equipment (RP-1173). *HVAC&R Res., 12* (3), 429–449.

Shen, B., Braun, J.E., Groll, E.A. (2009). Improved methodologies for simulating unitary air conditioners at off-design conditions. *Int. J. Refrig., 32* (7), 1837–49.

Shen, B., Braun, J.E., Groll, E.A. (2011). The impact of refrigerant charge, airflow, and expansion devices on the measured performance of an air-source heat pump – Part I. *ASHRAE Trans., 117*, 533–551.

Wang, J., Gorbounov, M., Yasar, M., Reeve, H., Hjortland, A. L., Braun, J. E. (2016). Lab and Field Evaluation of Fault Detection and Diagnostics for Advanced Roof Top Unit. *Int. Refrig. Air Cond. Conf.* Paper 1590.

Wichman A., Braun J.E. (2009). Fault Detection and Diagnostics for Commercial Coolers and Freezers. *HVAC&R Res., 15* (1), 77-99.

Yoon, S.H., Payne,W.V., Domanski, P.A. (2011). Residential heat pump heating performance with single faults imposed. *Appl. Therm. Eng., 31* (5), 765–771.

ACKNOWLEDGEMENT

This work was supported by the Building America Program of the U.S. Department of Energy's Office of Energy Efficiency and Renewable Energy (EERE) under Building Technologies Office agreement DE-EE0008689. The heat pump was provided by AHRI. We are grateful to Dave Coziahr for his expertise and assistance with its installation.